# Solvable non-Hermitian skin effects and high-order exceptional points in real space

Xintong Zhang, Xiaoxiao Song, Shubo Zhang, Tengfei Zhang, Yuanjie Liao, Xinyi Cai, Jing Li<sup>†</sup>

Department of Optical Science and Engineering, Shanghai Ultra-Precision Optical Manufacturing Engineering Center, Fudan University, Shanghai 200438, China

E-mail: †lijing@fudan.edu.cn

February 2023

Abstract. Non-Hermitian systems can exhibit extraordinary boundary behaviors, called the non-Hermitian skin effects, where all the eigenstates are accumulated at the boundary of lattice. To give a full understanding and control of non-Hermitian skin effects, we develop an exact solution strategy to provide the analytical expression of solvable eigenvalues and eigenstates under open boundary condition, which is generally applicable for one-dimensional non-Hermitian open systems. The exact solution strategy enables us to analyze the condition of existence or non-existence of the non-Hermitian skin effects at a mathematically rigorous level. Additionally, the exact solution strategy allows us to search for the high-order exceptional points in real space. To illustrate our main results, we derive the exact solution for two examples, including the Su-Schrieffer-Heeger chain model with long-range couplings, and the ladder model with non-reciprocal interaction. Our exact solution strategy provides an efficient way to study various non-Hermitian phenomena.

Keywords non-Hermitian skin effects, exact solution, exceptional points

#### 1. Introduction

Non-Hermitian physics has attracted intensive studies since the discovery of parity-time symmetric systems which can provide entirely real spectrum without Hermiticity[1, 2], and the sufficient and necessary condition of the real spectrum is related to the pseudo-Hermiticity and quasi-Hermiticity[3, 4]. Actually, due to the non-equivalent energy exchange with the environment, the non-Hermitian Hamiltonian is useful to describe the realistic physical systems with complex spectrum, and the research on driven or dissipative open systems is on the rise in many fields, such as atomic and molecular physics[5], condensed matter physics[6], and mesoscopic physics[7]. Owing to the formal equivalence between wave equations and Schrödinger equation, many non-Hermitian classical systems have also been realized, such as photonics[8, 9, 10, 11, 12], electrical circuits[13, 14, 15, 16, 17], acoustics[18, 19], and magnetics[20, 21]. One of the most significant characters of non-Hermitian systems is the exceptional point[22, 23], where the degeneracy of eigenvalues always comes along with the degeneracy of eigenstates, beyond any known phenomenon from their Hermitian counterparts, thus providing the potential application in the enhancement of sensitivity[24].

In recent years, the interplay between non-Hermitian physics and topological physics also brings out new phenomena in non-Hermitian systems [25, 26, 27, 28]. The traditional band topology can date back to the discovery of integer quantum Hall effect [29, 30, 31]. As is well-known for Hermitian systems, a nontrivial Bloch band invariant implies the emergence of topological edge states under open boundary However, similar bulk-boundary correspondence appears to be condition [32, 33]. violated in non-Hermitian systems. On one hand, the spectrum under open boundary condition is far different from that under periodical boundary condition, particularly, the topological phase transition points are not equivalent to the bulk gap-closing points[34, 35], and the traditional topological invariant cannot predict the topological edge states. On the other hand, such a non-consistency of spectra always comes along with a new phenomenon, called the non-Hermitian skin effects [35, 36, 37, 38, 39], where all the eigenstates for open systems are exponentially localized at the boundary of the lattice. Notably, the precondition of non-Hermitian skin effects relies on the fact that, unlike the Hermitian operators, the non-Hermitian operators only require that the right eigenvector is orthogonal to the left eigenvector [40]. However, the non-Hermitian skin effects cannot be predicted by the conventional topological invariant.

Several efforts have been made to predict the non-Hermitian skin effects, and restore the bulk-boundary correspondence in non-Hermitian systems. For example, the well-known generalized Brillouin Zone (GBZ) method[41, 35, 42, 43, 44] can predict the non-Hermitian skin effects by the calculation on the generalized Brillouin Zone. Additionally, the transfer-matrix method[45] can also explain the correspondence between the non-Hermitian skin effects and the non-consistency of spectra, by the derivation of transfer matrix. Furthermore, the exact solution strategy is proposed to provide the analytical expression of the non-Hermitian skin modes[46, 47, 48]. Here, we prefer the exact

solution strategy, because it can give us a direct understanding and full control of non-Hermitian skin effects, and formulate the bulk-boundary correspondence at a mathematically rigorous level. It has been reported that the exact solution strategy is effective for several one-dimensional and two-dimensional Hermitian systems, where it is known as the generalized Bloch theorem[49, 50]. While in non-Hermitian regime, the exact solution strategy has only been proved valid in one-dimensional model with short-range couplings. It is still challenging to extend the exact solution strategy for more complicated non-Hermitian models.

In this work, we address this issue by the development on exact solution strategy for general one-dimensional non-Hermitian models, and show how it can give us a direct and full understanding of various non-Hermitian phenomena. In Sec 2, we illustrate the main steps of our exact solution strategy for a generic one-dimensional non-Hermitian tight-binding model with sub-lattice symmetry, and provide the extended version to be applicable for arbitrary one-dimensional model. Compared with relative works, our main contribution relies on the derivation of Vieta's formulas, which relates the roots and the coefficients of the characteristic equation with arbitrary degree. In Sec 3, we take two concrete examples, Su-Schrieffer-Heeger (SSH) chain model with long-range couplings, and a more complicated model called ladder model, to demonstrate how the exact solution strategy helps us conveniently analyze the condition of existence or non-existence of non-Hermitian skin effects at a mathematically rigorous level. In Sec 4, the exact solution strategy can also allow us to search for the real-space high-order exceptional points, which is unique to non-Hermitian open systems. Additionally, we discuss about the connection between the exact solution strategy and the generalized Brillouin Zone method in Sec 5. Our exact solution strategy provides an efficient way to study various non-Hermitian phenomena.

## 2. Exact Solution strategy for non-Hermitian open systems

To demonstrate the exact solution strategy for non-Hermitian open systems, we start from a generic one-dimensional tight-binding lattice model protected by sub-lattice symmetry. The second-quantized Hamiltonian  $\hat{H}$  in real space is written as,

$$\hat{H} = \sum_{n=1}^{N} \varepsilon_{0} (c_{n,A}^{\dagger} c_{n,A} + c_{n,B}^{\dagger} c_{n,B}) + t_{0L} c_{n,A}^{\dagger} c_{n,B} + t_{0R} c_{n,B}^{\dagger} c_{n,A}$$

$$+ \sum_{m=1}^{M} \sum_{n=1}^{N-m} \sum_{i=A,B} \sum_{j=A,B} t_{m,R}^{i,j} c_{n+m,i}^{\dagger} c_{n,j} + t_{m,L}^{i,j} c_{n,j}^{\dagger} c_{n+m,i},$$

$$(1)$$

where N is the total number of unit cells, and  $c_{n,A/B}^{\dagger}(c_{n,A/B})$  denotes the creation (annihilation) operator of A or B site on the  $n^{\text{th}}$  cell, n=1,..,N. The first summation term in equation (1) consists of the on-site term with the same energy  $\varepsilon_0$  for both sites, and the intra-cell interaction with non-reciprocal hopping parameters  $t_{0L}, t_{0R}$ . While the second term in equation (1) represents the inter-cell interaction with non-reciprocal

hopping parameters  $t_{m,R}$  ( $t_{m,L}$ ) along right (left) direction, where m represents the  $m^{\text{th}}$ -nearest cells, and at most  $M^{\text{th}}$ -nearest inter-cell interaction is considered. Open boundary condition induced in the lattice model is defined as the hopping truncation between the  $k^{\text{th}}$  cell and the  $N-M+k,...,N^{\text{th}}$  cell, where k=1,...,M.

The first step of the exact solution strategy is to separate the whole open system into bulk subsystem and boundary subsystem, thus the eigenvalue equation  $\hat{H}|\Psi\rangle = E|\Psi\rangle$  under open boundary condition is split into the bulk equation and boundary equation. Rewrite the eigenstates of open system as  $|\Psi\rangle = \sum_{n=1}^{N} \phi_{n,A} c_{n,A}^{\dagger} |0\rangle + \phi_{n,B} c_{n,B}^{\dagger} |0\rangle$ , where  $\phi_{n,A/B}$  is the amplitude on the  $n^{\text{th}}$  cell, and then the bulk equation can be expressed as,

$$t_{0L}\phi_{n,B} + \sum_{m=1}^{M} \left(\sum_{j=A,B} t_{m,R}^{A,j}\phi_{n-m,j} + \sum_{i=A,B} t_{m,L}^{i,A}\phi_{n+m,i}\right) = (E - \varepsilon_0)\phi_{n,A},$$

$$t_{0R}\phi_{n,A} + \sum_{m=1}^{M} \left(\sum_{j=A,B} t_{m,R}^{B,j}\phi_{n-m,j} + \sum_{i=A,B} t_{m,L}^{i,B}\phi_{n+m,i}\right) = (E - \varepsilon_0)\phi_{n,B},$$
(2)

where n=M+1,...,N-M. As a generalization of Bloch states under periodical boundary condition, a possible ansatz of the eigenstates under open boundary condition should be expressed as  $\phi_{n,A} = \phi_A z^n$  and  $\phi_{n,B} = \phi_B z^n$ , where  $z \in \mathbb{C}$  and  $\phi_A, \phi_B$  denote the scaling factors. Therefore, if  $E \neq \varepsilon_0$ , the bulk equation in equation (2) is transformed into a 4M-degree equation about z, namely, characteristic equation,

$$(t_{0L} + \sum_{m=1}^{M} t_{m,R}^{A,B} z^{-m} + t_{m,L}^{B,A} z^{m})(t_{0R} + \sum_{m=1}^{M} t_{m,R}^{B,A} z^{-m} + t_{m,L}^{A,B} z^{m})$$

$$= (E - \varepsilon_{0} - \sum_{m=1}^{M} t_{m,R}^{A,A} z^{-m} + t_{m,L}^{A,A} z^{m})(E - \varepsilon_{0} - \sum_{m=1}^{M} t_{m,R}^{B,B} z^{-m} + t_{m,L}^{B,B} z^{m}).$$
(3)

Next, the characteristic equation can be expanded to a polynomial equation written as,

$$\omega_0 z^{4M} - \omega_1 z^{4M-1} + \omega_2 z^{4M-2} -, \dots, -\omega_{4M-1} z + \omega_{4M} = 0, \ (\omega_0 \neq 0),$$
 (4)

where the coefficients  $\omega_{1,...,4M}$  are dependent on the hopping parameters or eigenvalues E. According to the Vieta's theorem, the roots of characteristic equation  $\{z_1, z_2, ..., z_{4M}\}$  have the relation with  $\omega_{1,...,4M}$ ,

$$z_{1} + z_{2} + \dots + z_{4M} = \frac{\omega_{1}}{\omega_{0}},$$

$$z_{1}z_{2} + z_{1}z_{3} + \dots + z_{4M-1}z_{4M} = \frac{\omega_{2}}{\omega_{0}},$$

$$z_{1}z_{2}z_{3} + z_{1}z_{2}z_{4} + \dots + z_{4M-2}z_{4M-1}z_{4M} = \frac{\omega_{3}}{\omega_{0}},$$

$$\dots$$

$$z_{1}z_{2} + \dots + z_{4M} = \frac{\omega_{4M}}{\omega_{0}}.$$
(5)

The relation described in equation (5) works as a crucial step in the exact solution strategy. We will show you later that, how the Vieta's formulas efficiently help us analyze

the extraordinary non-Hermitian phenomena, e.g., the existence or non-existence of non-Hermitian skin effects in Sec 3, and the appearance of real-space high-order exceptional points in Sec 4.

Next, we discuss how the open boundary conditions constrain the value range of the roots  $\{z_1, z_2, ..., z_{4M}\}$ . Combined with the bulk equation described in equation (2), the boundary equation split from the eigenvalue equation is simplified as,

$$\phi_{N+1,A} = 0, \ \phi_{0,B} = 0, \tag{6}$$

which means, for open systems with finite lattice size, the amplitude outside the lattice is truncated. Since the characteristic equation have 4M roots, the ansatz of eigenstates should be revised as  $\phi_{n,A} = \sum_{i=1}^{4M} \phi_A^{(i)} z^n$  and  $\phi_{n,B} = \sum_{i=1}^{4M} \phi_B^{(i)} z^n$ , thus the boundary equation shown in equation (6) becomes,

$$\sum_{i=1}^{4M} \phi_A^{(i)} z_i^{N+1} = 0, \ \sum_{i=1}^{4M} \phi_B^{(i)} = 0.$$
 (7)

Let  $\phi_B^{(i)} = \Gamma_i \phi_A^{(i)}$ , where  $\Gamma_i$  is derived from the bulk equation in equation (2), and then the boundary equation in equation (7) becomes,

$$\begin{pmatrix} z_1^{N+1} & z_2^{N+1} & \cdots & z_{4M}^{N+1} \\ \Gamma_1 & \Gamma_2 & \cdots & \Gamma_{4M} \end{pmatrix} \begin{pmatrix} \phi_A^{(1)} \\ \phi_A^{(2)} \\ \vdots \\ \phi_A^{(4M)} \end{pmatrix} = \mathbf{0}.$$
 (8)

Therefore, the non-trivial solution of the scaling factors  $\{\phi_A^{(1)}, \phi_A^{(2)}, ..., \phi_A^{(4M)}\}$  exists if and only if

$$\exists z_1, z_2, \ z_1^{N+1} \Gamma_2 = z_2^{N+1} \Gamma_1, \tag{9}$$

where  $\phi_A^{(1),(2)} \neq 0$  and  $\phi_A^{(3),\dots,(4M)} = 0$ . There are only two components  $z_1^n$  and  $z_2^n$  that can survive in the expression of possible eigenstates, and  $z_1, z_2$  must be a pair of complex roots to guarantee equation (9) is still satisfied under the thermodynamic limit that  $N \to \infty$ . Rewrite the form of the complex pair as  $z_1 = e^{\alpha + i\theta}$  and  $z_2 = e^{\alpha - i\theta}$ , where  $\alpha \in \mathbb{R}$  and  $\theta \in (0, \pi)$ . Finally, the Vieta's formulas derived from the bulk equation, and the open boundary condition derived from the boundary equation jointly decide the value of  $\alpha$  and  $\theta$ . In next section we will see that, benefiting from the induction of  $\alpha$  and  $\theta$ , it is of great convenience to display the expression of eigenvalues and eigenstates in non-Hermitian open systems.

The exact solution strategy can also be extended to more complicated onedimensional models. For example, if the sub-lattice symmetry is broken, the bulk equation and characteristic equation should be revised accordingly. Furthermore, if each unit cell contains S sites, the characteristic equation will become a 2MS-degree polynomial equation, where the Vieta's theorem is still effective. The open boundary condition requires that the determinant of a  $S \times S$  matrix is equal to zero, so there will be S components of  $z^n$  that can survive in the expression of eigenstates. Therefore, our exact solution strategy is generally applicable for one-dimensional non-Hermitian models.

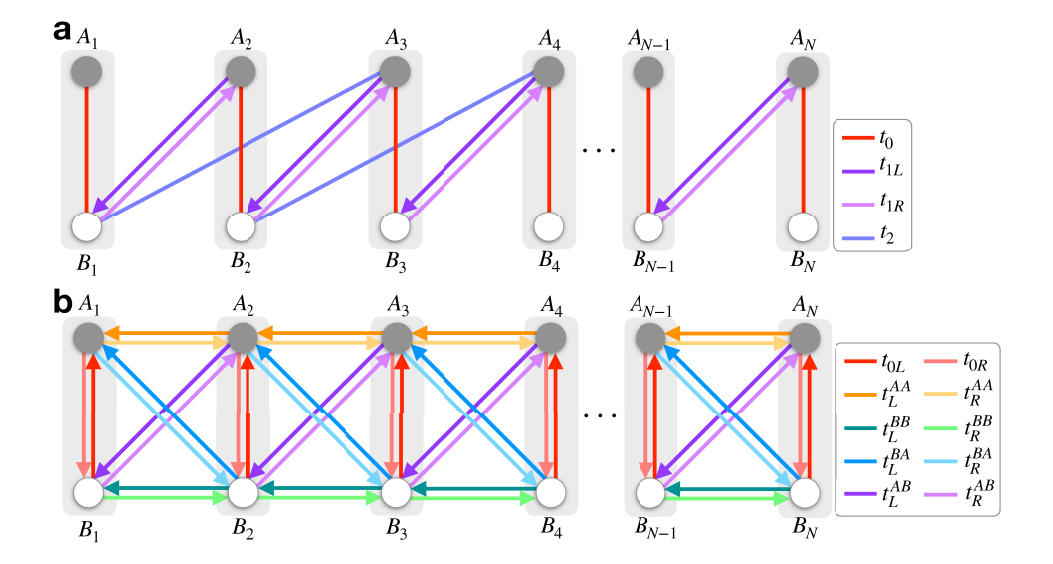


Figure 1. Schematic views of the one-dimensional non-Hermitian tight-binding models under open boundary conditions. (a) Non-Hermitian SSH chain model with long-range couplings. (b) Ladder model with 5 pairs of non-reciprocal hopping terms.

# 3. Non-Hermitian skin effects and pseudo-Hermitian symmetry

#### 3.1. SSH chain model with long-range couplings

To illustrate our main results, we now discuss two concrete and instructive examples. As shown in figure 1(a), the first example is the SSH chain model with long-range couplings, where the hopping parameters described in equation (1) are reduced into  $t_{0L} = t_{0R} = t_0$ ,  $t_{1,R}^{A,B} = t_{1R}$ ,  $t_{1,L}^{A,B} = t_{1L}$  and  $t_{2,L}^{A,B} = t_{2,R}^{A,B} = t_2$ . The real-space Hamiltonian of the SSH chain model under open boundary condition is written as,

$$\hat{H} = \sum_{n=1}^{N} \varepsilon_0 (c_{n,A}^{\dagger} c_{n,A} + c_{n,B}^{\dagger} c_{n,B}) + t_0 (c_{n,A}^{\dagger} c_{n,B} + c_{n,B}^{\dagger} c_{n,A})$$

$$+ \sum_{n=1}^{N-1} t_{1R} c_{n+1,A}^{\dagger} c_{n,B} + t_{1L} c_{n,B}^{\dagger} c_{n+1,A} + \sum_{n=1}^{N-2} t_2 (c_{n+2,A}^{\dagger} c_{n,B} + c_{n,B}^{\dagger} c_{n+2,A}).$$

$$(10)$$

Correspondingly, the characteristic equation of the SSH chain model is a quartic polynomial equation written as,

$$\omega_{0}z^{4} - \omega_{1}z^{3} + \omega_{2}z^{2} - \omega_{3}z + \omega_{4} = 0,$$

$$\omega_{0} = t_{0}t_{2},$$

$$\omega_{1} = -(t_{0}t_{1L} + t_{1R}t_{2}),$$

$$\omega_{2} = t_{0}^{2} + t_{1L}t_{1R} + t_{2}^{2} - (E - \varepsilon_{0})^{2},$$

$$\omega_{3} = -(t_{0}t_{1R} + t_{1L}t_{2}),$$

$$\omega_{4} = t_{0}t_{2}.$$
(11)

Assuming that  $\omega_0, \omega_4 \neq 0$ , the four roots and the coefficients of the characteristic

equation have the relation described by Vieta's formulas,

$$z_{1} + z_{2} + z_{3} + z_{4} = \frac{\omega_{1}}{\omega_{0}},$$

$$z_{1}z_{2} + z_{1}z_{3} + z_{1}z_{4} + z_{2}z_{3} + z_{2}z_{4} + z_{3}z_{4} = \frac{\omega_{2}}{\omega_{0}},$$

$$z_{1}z_{2}z_{3} + z_{1}z_{2}z_{4} + z_{1}z_{3}z_{4} + z_{2}z_{3}z_{4} = \frac{\omega_{3}}{\omega_{0}},$$

$$z_{1}z_{2}z_{3}z_{4} = \frac{\omega_{4}}{\omega_{0}}.$$

$$(12)$$

As mentioned in Sec 2, a pair of complex roots  $z_1 = e^{\alpha + i\theta}$  and  $z_2 = e^{\alpha - i\theta}$  must exist by the constraint of open boundary condition. Therefore, another two roots of the characteristic equation should be written as  $z_3 = e^{-\alpha + \lambda}$  and  $z_4 = e^{-\alpha - \lambda}$  with  $\lambda \in \mathbb{C}$ , because  $z_1 z_2 z_3 z_4 = 1$  in the SSH chain model.

Next, we discuss about how exactly the open boundary condition constraints the value of the roots in the characteristic equation. According to equation (9), the boundary equation requires that  $z_1^{N+1}\Gamma_2 = z_2^{N+1}\Gamma_1$ , where  $\Gamma_i$  is the ratio between  $\phi_A^{(i)}$  and  $\phi_B^{(i)}$ ,

$$\Gamma_i = \frac{E - \varepsilon_0}{t_0 + t_{1R} z_i^{-1} + t_2 z_j^{-2}}.$$
(13)

Therefore, the relation between  $z_1$  and  $z_2$  is derived as,

$$t_0(z_1^{N+1} - z_2^{N+1}) + t_{1R}(z_1^N - z_2^N) + t_2(z_1^{N-1} - z_2^{N-1}) = 0.$$
(14)

Benefiting from the induction of  $\alpha$  and  $\theta$ , the open boundary condition in equation (14) is further simplified as,

$$\sin[(N+1)\theta] + \mu_1 \sin[N\theta] + \mu_2 \sin[(N-1)\theta] = 0, \tag{15}$$

where  $\mu_1 = e^{-\alpha}t_{1R}/t_0$ ,  $\mu_2 = e^{-2\alpha}t_2/t_0$ . Although  $\theta$  cannot be analytically solved from the open boundary condition, an essential fact is discovered that under the thermodynamic limit  $N \to \infty$ , the value of  $\theta$  is continuous within  $(0, \pi)$ .

Consequently, the crucial step of the exact solution strategy focuses on how the eigenvalues and eigenstates can be analytically expressed as the function of  $\theta$ . To handle this problem, we need to induce  $\alpha$ ,  $\theta$ ,  $\lambda$  into the Vieta's formulas shown in equation (12),

$$2e^{\alpha}\cos\theta + 2e^{-\alpha}\cosh\lambda = \frac{\omega_1}{\omega_0},$$

$$2\cosh 2\alpha + 4\cos\theta\cosh\lambda = \frac{\omega_2}{\omega_0},$$

$$2e^{-\alpha}\cos\theta + 2e^{\alpha}\cosh\lambda = \frac{\omega_3}{\omega_0},$$
(16)

where  $\omega_2$  is related to the eigenvalues E, while  $\omega_0, \omega_1, \omega_3$  are only determined by the hopping parameters. Therefore, as long as  $\alpha \neq 0$ , the relation between  $\alpha$  and  $\theta$  is rigorously expressed as,

$$\cos \theta = \frac{\omega_1 e^{\alpha} - \omega_3 e^{-\alpha}}{2\omega_0 (e^{2\alpha} - e^{-2\alpha})}, \ \theta \in (0, \pi), \tag{17}$$

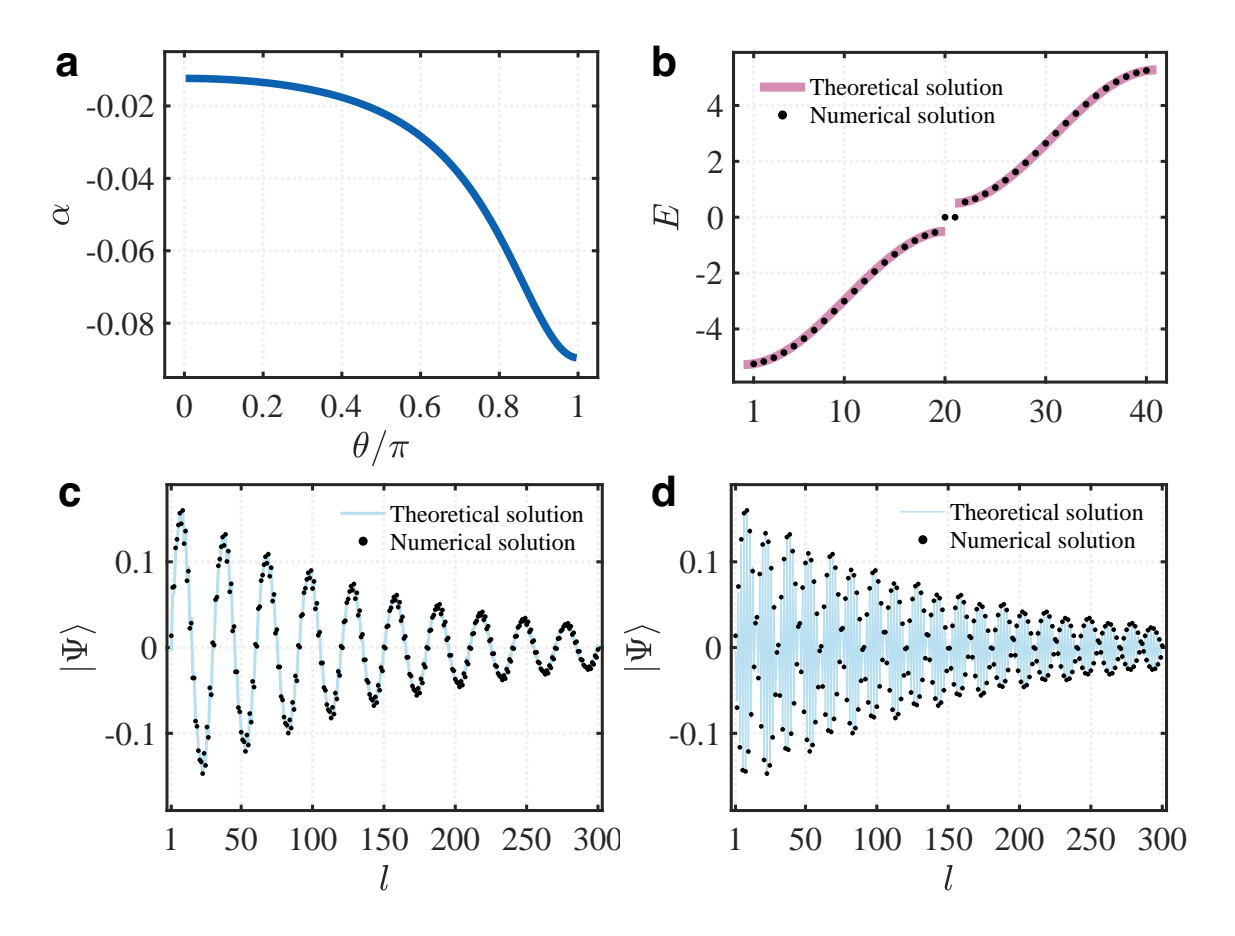


Figure 2. Results of exact solution strategy for SSH chain model under open boundary condition. (a) Localization parameter  $\alpha$  solved from  $\cos\theta = (\omega_1 \mathrm{e}^{\alpha} - \omega_3 \mathrm{e}^{-\alpha})/[2\omega_0(\mathrm{e}^{2\alpha} - \mathrm{e}^{-2\alpha})], \ \theta \in (0,\pi)$ . (b) Eigenvalues E and (c,d) eigenstates  $|\Psi\rangle$ , where the solid lines represent the theoretical solution derived from our exact solution strategy, and the dots represent the numerical solution calculated from the diagonalization of Hamiltonian matrix. l represents the  $l^{\text{th}}$  site in the one-dimensional chain. The hopping parameters are set as  $\varepsilon_0 = 0$ ,  $t_0 = 1$ ,  $t_{1L} = 2.5$ ,  $t_{1R} = 3.5$  and  $t_2 = 1.3$ .

where  $\theta$  is regarded as a given variable under the thermodynamic limit, as shown in figure 2(a). Meanwhile, the relation between  $\alpha$  and  $\lambda$  is rigorously expressed as,

$$\cosh \lambda = \frac{\omega_3 e^{\alpha} - \omega_1 e^{-\alpha}}{2\omega_0 (e^{2\alpha} - e^{-2\alpha})}.$$
(18)

Finally, the solvable eigenvalue E of the SSH chain model is analytically expressed as a function of  $\alpha(\theta)$ ,

$$E = \varepsilon_0 \pm \sqrt{t_0^2 + t_{1L}t_{1R} + t_2^2 - t_0t_2(2\cosh 2\alpha + \frac{2\omega_1\omega_3\cosh 2\alpha - \omega_1^2 - \omega_3^2}{4\omega_0^2\sinh^2 2\alpha})}.(19)$$

Additionally, the eigenstate can also be expressed as a function of  $\alpha$  and  $\theta$ . Since  $\phi_B^{(1)} = \Gamma_1 \phi_A^{(1)}$ ,  $\phi_B^{(2)} = \Gamma_2 \phi_A^{(2)}$ , and  $\phi_B^{(1)} + \phi_B^{(2)} = 0$ , the eigenstates  $\phi_{n,A}$  and  $\phi_{n,B}$  should be

derived as,

$$\phi_{n,A} = \phi_A^{(1)} z_1^n + \phi_A^{(2)} z_2^n$$

$$= \phi_A^{(1)} (z_1^n - \frac{\Gamma_1}{\Gamma_2} z_2^n)$$

$$= \phi_0 e^{\alpha n} (\sin[n\theta] + \mu_1 \sin[(n-1)\theta] + \mu_2 \sin[(n-2)\theta]),$$
(20)

$$\phi_{n,B} = \phi_B^{(1)} z_1^n + \phi_B^{(2)} z_2^n$$

$$= \Gamma_1 \phi_A^{(1)} (z_1^n - z_2^n)$$

$$= \phi_0 (E - \varepsilon_0) e^{\alpha n} \sin[n\theta],$$
(21)

where  $\phi_0 = 2i\phi_A^{(1)}t_0/(t_0 + t_{1R}z_1^{-1} + t_2z_1^{-2})$ , and  $\theta \in (0, \pi)$  under the thermodynamic limit that  $N \to \infty$ .

The analytical expression of eigenstates illustrates that, the solvable eigenstates with  $E \neq \varepsilon_0$  are entirely evolved from the bulk states under periodical boundary condition, modified by  $e^{\alpha n}$  in the real space, where  $\alpha$  is the localization parameter. As long as  $\alpha \neq 0$ , all of the solvable eigenstates are localized at the boundary of lattice model, which is the so called non-Hermitian skin effects. When  $\alpha < 0$ , the skin modes are localized at n = 1 side with penetration length  $-1/\alpha$ , while when  $\alpha > 0$ , the skin modes are localized at n = N side with penetration length  $1/\alpha$ . To prove the validity of the exact solution strategy, the numerical solutions of eigenvalues and eigenstates are also calculated through the diagonalization of Hamiltonian matrix. As shown in figures 2(b,c,d), the numerical solution and the theoretical solution correspond to each other precisely.

Many relative works have discovered that, the non-Hermitian skin effect is a very universal phenomenon in non-Hermitian open systems. However, we need pay more attention on a special case that non-Hermitian systems cannot exhibit non-Hermitian skin effects. A typical system is the parity-time symmetric system with balanced gain and loss, and it can provide relatively stable states in realistic non-Hermitian systems[15], which is beneficial to some practical application. Here, our exact solution strategy is very efficient to analyze the non-existence of non-Hermitian skin effects. It requires that, for arbitrary  $\theta$ , the localization parameter  $\alpha$  is always equal to zero, and then all of the solvable eigenstates behave like the bulk states without localization. Inducing  $\alpha = 0$  into the Vieta's formulas described in equation (16), then we get,

$$2\cos\theta + 2\cosh\lambda = \frac{\omega_1}{\omega_0},$$

$$2\cos\theta + 2\cosh\lambda = \frac{\omega_3}{\omega_0}.$$
(22)

Therefore, the non-Hermitian skin effects vanish if and only if  $\omega_1 = \omega_3$ , that is,  $t_{1L} = t_{1R}$  or  $t_0 = t_2$ . The former becomes the Hermitian case, while the latter is still the non-Hermitian case, but the intra-cell interaction  $t_0$  is equal to the long-range inter-cell interaction  $t_2$ . Symmetry plays a significant role on the non-existence of non-Hermitian

skin effects. When  $t_0 = t_2$ , the Bloch Hamiltonian of the SSH chain model is protected by the pseudo-Hermitian symmetry [51], described as

$$H^{\dagger} = \rho H \rho^{-1},\tag{23}$$

where the pseudo-Hermiticity operator  $\rho$  is a Hermitian and invertible matrix. More details on the proof of pseudo-Hermitian symmetry in the SSH chain model are illustrated in Appendix A.

## 3.2. Ladder model with non-reciprocal interaction

To demonstrate that the mentioned benefits of our exact solution strategy are generally applicable, a more complicated one-dimensional lattice model is proposed. As shown in figure 1(b), the second example is modified from Lee's model[34], here we call it ladder model, where each site is coupled with 5 neighboring sites, and the hopping terms between sites are non-reciprocal, leading to 10 degrees of freedom. According to the derivation of exact solution strategy shown from equation (1) to equation (5), the characteristic equation of the ladder mode is written as,

$$\omega_{0}z^{4} - \omega_{1}z^{3} + \omega_{2}z^{2} - \omega_{3}z + \omega_{4} = 0, \quad (\omega_{0} \neq 0)$$

$$\omega_{0} = t_{L}^{AA}t_{L}^{BB} - t_{L}^{AB}t_{L}^{BA},$$

$$\omega_{1} = (E - \varepsilon_{0})(t_{L}^{AA} + t_{L}^{BB}) + t_{0L}t_{L}^{AB} + t_{0R}t_{L}^{BA},$$

$$\omega_{2} = (E - \varepsilon_{0})^{2} + t_{L}^{AA}t_{R}^{BB} + t_{L}^{BB}t_{R}^{AA} - t_{0L}t_{0R} - t_{L}^{AB}t_{R}^{AB} - t_{L}^{BA}t_{R}^{BA},$$

$$\omega_{3} = (E - \varepsilon_{0})(t_{R}^{AA} + t_{R}^{BB}) + t_{0L}t_{R}^{BA} + t_{0R}t_{R}^{AB},$$

$$\omega_{4} = t_{R}^{AA}t_{R}^{BB} - t_{R}^{AB}t_{R}^{BA}.$$
(24)

The open boundary condition requires that  $z_1 = e^{\alpha + i\theta}$ ,  $z_2 = e^{\alpha - i\theta}$ , and then  $z_3 = e^{\beta + \lambda}$  and  $z_4 = e^{\beta - \lambda}$ , where  $\alpha, \beta \in \mathbb{R}, \theta \in (0, \pi), \lambda \in \mathbb{C}$ . Therefore, the Vieta's formulas expressed by  $\alpha, \theta, \beta, \lambda$  should be derived as,

$$2e^{\alpha}\cos\theta + 2e^{\beta}\cosh\lambda = \frac{\omega_1}{\omega_0},$$

$$e^{2\alpha} + e^{2\beta} + 4e^{\alpha+\beta}\cos\theta\cosh\lambda = \frac{\omega_2}{\omega_0},$$

$$2e^{\alpha+2\beta}\cos\theta + 2e^{2\alpha+\beta}\cosh\lambda = \frac{\omega_3}{\omega_0},$$

$$e^{2\alpha+2\beta} = \frac{\omega_4}{\omega_0}.$$
(25)

To analyze the non-existence of non-Hermitian skin effects in the ladder model, we insert  $\alpha = 0$  into the Vieta's formulas, and then,

$$\forall \theta \in (0, \pi), 2\cos\theta(\omega_0 - \omega_4) = \omega_1 - \omega_3. \tag{26}$$

Consequently, the non-Hermitian skin effects vanish if and only if  $\omega_0 = \omega_4$  and  $\omega_1 = \omega_3$  are simultaneously satisfied, which means,

$$\begin{cases}
t_L^{AA} t_L^{BB} - t_L^{AB} t_L^{BA} = t_R^{AA} t_R^{BB} - t_R^{AB} t_R^{BA} \\
t_L^{AA} + t_L^{BB} = t_R^{AA} + t_R^{BB} \\
t_{0L} t_L^{AB} + t_{0R} t_L^{BA} = t_{0L} t_R^{BA} + t_{0R} t_R^{AB}
\end{cases}$$
(27)

Otherwise, the non-Hermitian skin effects can definitely appear in the ladder model under open boundary condition. As shown in figure 3, except for topological edge states, all the eigenstates are localized when  $t_L^{AB} = 1.1$ , while when  $t_L^{AB} = 0.5$ , the eigenstates behaves like the bulk states, which is consistent with the analytical results described in equation (27). Therefore, our exact solution strategy provides an efficient and general way to rigorously analyze the existence or non-existence of non-Hermitian skin effects.

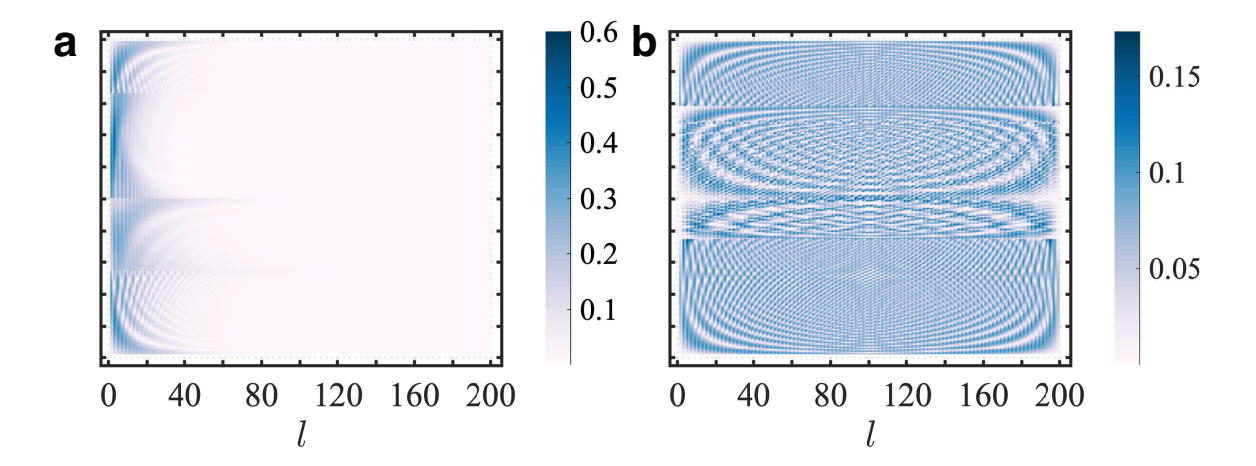


Figure 3. Absolute values of the eigenstates for ladder model under open boundary condition. (a) Case without pseudo-Hermitian symmetry. (b) Case with pseudo-Hermitian symmetry. The hopping parameters are set as  $\varepsilon_0=0$ ,  $t_{0L}=1$ ,  $t_{0R}=0.5$ ,  $t_L^{AA}=1.2$ ,  $t_R^{AA}=0.6$ ,  $t_L^{BB}=0.6$ ,  $t_R^{BB}=1.2$ ,  $t_R^{AB}=1$ ,  $t_L^{BA}=3$ ,  $t_R^{BA}=1.5$ ,  $t_L^{AB}=1.1$  in (a) and  $t_L^{AB}=0.5$  in (b).

## 4. Real-space high-order exceptional points

In this section, another extraordinary non-Hermitian phenomenon is discovered in the non-Hermitian SSH chain model and ladder model, called the real-space high-order exceptional points (EPs). Similar to the definition of momentum-space EPs under periodical boundary conditions, the real-space EPs appear when both the eigenvalues and eigenvectors coalesce under open boundary conditions, which is unique to non-Hermitian open systems. Also known as high-order EPs, the degeneracy of real-space EPs increases with the scaling of lattice size, leading to a significant enhancement of sensitivity. Therefore, to utilize these advantages for future practical application, the full understanding and control of real-space high-order EPs is of great significance.

The exact solution strategy enables us to search the real-space EPs rigorously and completely. It has been reported that, the eigenstates of real-space EPs are pinned at the terminal of lattice model[45], regarded as an extreme case of non-Hermitian skin effects. Inspired by this association, we deduced that the real-space EPs appear as long as the localization parameter satisfies  $\alpha = \mp \infty$ , to guarantee that the eigenstates are

pinned at the n=1 terminal or n=N terminal. Here, by inserting  $\alpha=\mp\infty$ , the Vieta's formulas described in equation (16) for the SSH chain model becomes,

$$\mathcal{O}(z) = -\frac{t_0 t_{1L} + t_{1R} t_2}{t_0 t_2},$$

$$\mathcal{O}(z^2) = \frac{t_0^2 + t_{1L} t_{1R} + t_2^2 - (E - \varepsilon_0)^2}{t_0 t_2},$$

$$\mathcal{O}(z) = -\frac{t_0 t_{1R} + t_{1L} t_2}{t_0 t_2},$$
(28)

where  $\mathcal{O}(z^x)$  represents x-order infinitely large quantity. Therefore, one possible way is to let  $t_0 = 0$  and  $t_{1L} = 0$ . Fortunately, now the SSH chain model can be entirely solvable directly from the eigenvalue equation  $\hat{H}|\Psi\rangle = E|\Psi\rangle$ . As shown in figure 4, when  $t_0 = 0$  and  $t_{1L} = 0$ , the number of topological edge states is 4, and two real-space EPs with order N-2 appear, where the eigenvalues and eigenstates are analytically expressed as,

$$E_{\pm} = \varepsilon_0 \pm t_2, \ |\Psi_{\pm}\rangle = [0, \pm 1, t_{1R}/t_2, 0, 1, 0, 0, ..., 0]^{\mathrm{T}}.$$
 (29)

When  $t_0=0$  and  $t_{1L}=0$ , it looks like the hopping terms along right direction is entirely truncated, so the eigenstates are strongly accumulated at n=1 terminal. Similarly, when  $t_0=0$  and  $t_{1R}=0$ , two N-2 fold real-space EPs appears, where the eigenstates are accumulated at n=N terminal because the hopping along left direction is truncated. Furthermore, the condition  $t_2=0, t_{1L}=0$ , or  $t_2=0, t_{1R}=0$  also displays two N-fold real-space EPs, and totally four cases of real-space EPs are found through the exact solution strategy, as shown in Table 1.

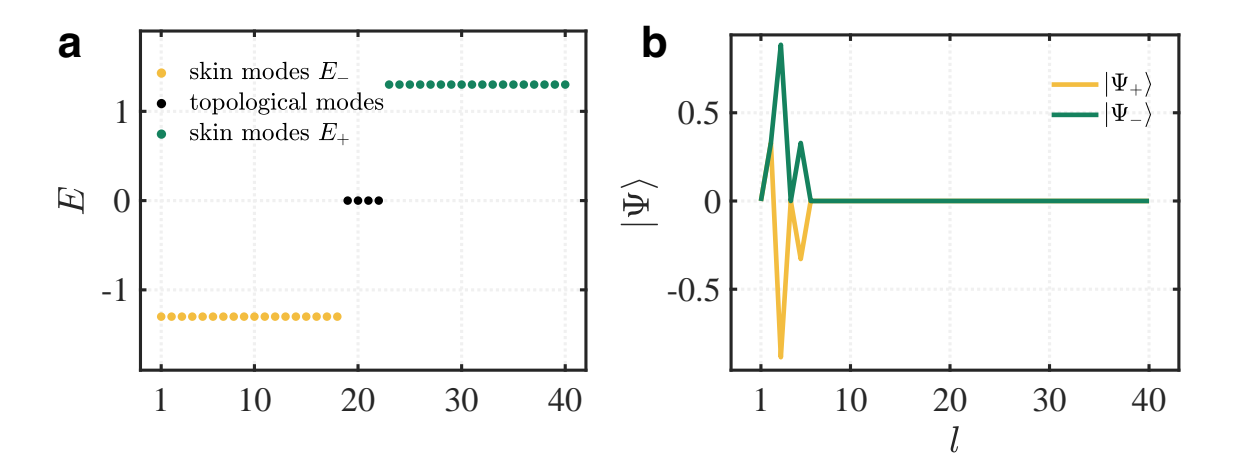


Figure 4. Exact solution to the (a) eigenvalues and (b) eigenstates at real-space high-order exceptional point for SSH chain model. The hopping parameters are set as  $\varepsilon_0 = 0$ ,  $t_0 = 0$ ,  $t_{1L} = 0$ ,  $t_{1R} = 3.5$ , and  $t_2 = 1.3$ .

The exact solution strategy is also applicable for the ladder model to analyze the real-space high-order EPs. Obviously, as shown in Table 1, the point at  $t_L^{AA} = t_L^{BB} = t_L^{AB} = t_L^{BA} = 0$  or  $t_R^{AA} = t_R^{BB} = t_R^{AB} = t_R^{BA} = 0$  is definitely a real-space EP, because every inter-cell hopping term along left/right direction vanish. More

Model	Parameters	Order	Eigenvalues	Eigenstates
	$t_0 = 0, t_{1L} = 0$ $t_0 = 0, t_{1R} = 0$ $t_2 = 0, t_{1L} = 0$ $t_2 = 0, t_{1R} = 0$	N-2	$\varepsilon_0 \pm t_2$ $\varepsilon_0 \pm t_2$ $\varepsilon_0 \pm t_0$ $\varepsilon_0 \pm t_0$	$ \begin{bmatrix} [0, \pm 1, t_{1R}/t_2, 0, 1, 0, 0,, 0]^{\mathrm{T}} \\ [0,, 0, 0, 1, 0, t_{1L}/t_2, \pm 1, 0]^{\mathrm{T}} \\ [0,, 0, 0, \pm 1, 1]^{\mathrm{T}} \\ [1, \pm 1, 0, 0,, 0]^{\mathrm{T}} $
ladder model	$t_{R}^{AA}t_{R}^{BB} - t_{R}^{AB}t_{R}^{BA} = 0,$		$arepsilon_0 \pm \sqrt{E_L}$	$[0,,0,0,\pm \frac{\sqrt{t_{0L}t_{0R}}}{t_{0R}},1]^{\mathrm{T}}$ $[\frac{\sqrt{t_{0L}t_{0R}}}{t_{0R}},\pm 1,0,0,,0]^{\mathrm{T}}$ $[0,,0,0,\pm P_L,\pm Q_L,S_L,1]^{\mathrm{T}}$
	$t_R^{AA} + t_R^{BB} = 0, t_{0L}, t_{0R} = 0$	N-1	$\varepsilon_0 \pm \sqrt{E_R}$	$[\pm P_R, \pm Q_R, S_R, 1, 0, 0,, 0]^{\mathrm{T}}$

**Table 1.** High-order exceptional points in real space for SSH chain model and ladder model.

interestingly, the condition of real-space EPs in the ladder model is not so strict as that in SSH chain model. For example, assuming that  $t_L^{AA}$ ,  $t_L^{BB}$ ,  $t_L^{AB}$ ,  $t_L^{BA}$ ,  $t_L^{BA} \neq 0$ , we choose  $t_L^{AA}t_L^{BB} - t_L^{AB}t_L^{BA} = 0$ ,  $t_L^{AA} + t_L^{BB} = 0$ ,  $t_{0L} = t_{0R} = 0$  to let the coefficients  $\omega_0 = 0$  and  $\omega_1 = 0$ . The real-space eigenvalue equation of the ladder model is also entirely solvable under this condition. As shown in Table 1, the number of topological edge states is 2, while two N-1 fold real-space EPs appear, and their eigenvalues and eigenstates are analytically expressed as,

$$E_{\pm} = \varepsilon_0 \pm \sqrt{E_L}, |\Psi_{\pm}\rangle = [0, ..., 0, 0, \pm P_L, \pm Q_L, S_L, 1]^{\mathrm{T}},$$
(30)

where

$$E_{L} = [t_{L}^{AA}t_{L}^{AB}(t_{R}^{AA} - t_{R}^{BB}) + t_{L}^{AB^{2}}t_{R}^{AB} - t_{L}^{AA^{2}}t_{R}^{BA}]/t_{L}^{AB},$$

$$P_{L} = \sqrt{E_{L}}t_{L}^{AA}/(t_{L}^{AA}t_{R}^{BA} + t_{L}^{AB}t_{R}^{BB}),$$

$$Q_{L} = \sqrt{E_{L}}t_{L}^{AB}/(t_{L}^{AA}t_{R}^{BA} + t_{L}^{AB}t_{R}^{BB}),$$

$$S_{L} = (t_{L}^{AA}t_{R}^{AA} + t_{L}^{AB}t_{R}^{ABB})/(t_{L}^{AA}t_{R}^{BA} + t_{L}^{AB}t_{R}^{BB}).$$
(31)

Although the inter-cell hopping terms  $t_L^{AA}$ ,  $t_L^{BB}$ ,  $t_L^{AB}$ ,  $t_L^{BA}$  along left direction still survive, their compensation of each other makes the total hopping between the nearest cells is stopped. Therefore, the eigenstates of real-space EPs are strongly accumulated at n=N terminal. Meanwhile, another case of real-space EP occurs when  $t_R^{AA}t_R^{BB} - t_R^{AB}t_R^{BA} = 0$ ,  $t_R^{AA} + t_R^{BB} = 0$ ,  $t_{0L} = t_{0R} = 0$ . In a brief summary, the exact solution strategy helps us discover more rich cases of real-space EPs in our non-Hermitian models, providing an effective way to fully understand and control the non-Hermitian open systems.

# 5. Exact solution to generalized Brillouin Zone

Besides from the analysis of non-Hermitian skin effects and real-space high-order exceptional points, our exact solution strategy is also helpful to improve the generalized Brillouin Zone method, which is a well-known method used to predict the non-Hermitian topological edge states and establish the non-Hermitian bulk-boundary correspondence. Firstly, we discuss about the connection between GBZ method and our exact solution strategy. The GBZ method has the same deduction that  $z_1, z_2$  must be a pair of complex roots by the constraint of open boundary condition, if sub-lattice symmetry is considered. Then, the energy E in the characteristic equation is regarded as a known constant, and through the parameter sweeping of E within a proper value range, a series of roots E can be numerically solved from characteristic equation. Therefore, only those E which can provide  $|z_1| = |z_2|$  are possible eigenvalues in the non-Hermitian open systems, and the loop of E in the complex plane are called the generalized Brillouin Zone E. The relation between the localization parameter E and the generalized Brillouin Zone E is written by,

$$\alpha = \log |\mathcal{C}|. \tag{32}$$

As shown in figure 5, the results of  $\mathcal{C}$  calculated from GBZ method and solved from our exact solution strategy are precisely consistent with each other. Since the localization parameter  $\alpha$  for our SSH chain model is not a constant with the change of  $\theta$ , the loop of generalized Brillouin Zone  $\mathcal{C}$  is not a circle in the complex plane. Our exact solution holds the advantage that the localization parameter  $\alpha$  is directly solved from equation (17), where  $\theta$  is regarded as a given variable under the thermodynamic limit. That is, unlike GBZ method, we do not need any information about the spectrum for open systems before calculating the loop of generalized Brillouin Zone, which is more convenient than traditional GBZ method, especially for the case with complex spectrum.

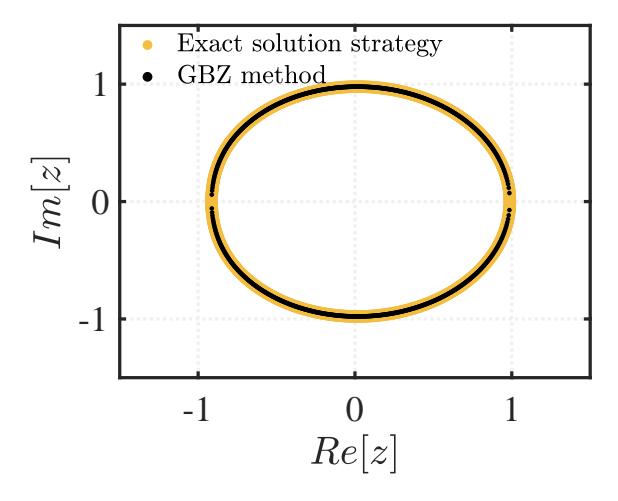


Figure 5. The loop of generalized Brillouin Zone in the complex plane for SSH chain model. The yellow dots denote the results derived from our exact solution strategy, where  $z = \mathrm{e}^{\alpha \pm \mathrm{i}\theta}, \theta \in (0,\pi)$ , while the black dots denote the results calculated from the generalized Brillouin Zone (GBZ) method. The hopping parameters are set as  $\varepsilon_0 = 0, t_0 = 1, t_{1L} = 2.5, t_{1R} = 3.5$  and  $t_2 = 1.3$ .

#### 6. Conclusions

In summary, we develop the exact solution strategy for general one-dimensional non-Hermitian models, and it becomes very convenient to analyze the extraordinary non-Hermitian phenomena. Through the derivation of the analytical expression of eigenstates for open systems, our exact solution strategy enables us to explore the non-Hermitian skin effects at a mathematically rigorous level. It demonstrates that all of the solvable eigenstates are evolved from the bulk states, and modified by an exponential term along one direction, where the localization parameter can be analytically solved. Pseudo-Hermitian symmetry plays a significant role on the non-existence of non-Hermitian skin effects. Furthermore, our exact solution strategy can help us analyze the high-order exceptional point in real space, and four cases of exceptional points are found in the SSH chain model and ladder model, respectively. Additionally, our exact solution strategy is helpful to improve the existing generalized Brillouin Zone method, and provides the analytical expression of generalized Brillouin Zone. Our exact solution strategy provides an efficient way to study various non-Hermitian phenomena.

# Acknowledgments

The authors thank for the support from the National Natural Science Foundation of China (Grant Nos. 60578047, 61427815), and the Natural Science Foundation of Shanghai (Grant Nos. 17ZR1402200, 13ZR1402600).

#### Data availability statement

The data that support the plots within this paper are available from the corresponding author on reasonable request.

## Appendix A. Definition of pseudo-Hermitian symmetry

Here, we give a proof that when  $t_0 = t_2$ , our SSH chain model is protected by the pseudo-Hermitian symmetry. The pseudo-Hermitian symmetry is defined as

$$H^{\dagger} = \rho H \rho^{-1} \tag{A.1}$$

where  $\rho$  is a Hermitian and invertible matrix. Assuming that  $\varepsilon_0 = 0$  and the hopping parameters are all real numbers, when  $t_0 = t_2$ , the Bloch Hamiltonian becomes

$$H(k) = \begin{pmatrix} 0 & h_a(k) \\ h_b(k) & 0 \end{pmatrix},$$

$$h_a(k) = e^{-ik} (t_{1R} + 2t_0 \cos k), \ h_b(k) = e^{ik} (t_{1L} + 2t_0 \cos k).$$
(A.2)

Therefore, the pseudo-Hermitian operator  $\rho$  should be written as

$$\rho = \begin{pmatrix} 0 & e^{-ik} \\ e^{ik} & 0 \end{pmatrix}. \tag{A.3}$$

According to Ref. [51], a canonical form of  $\rho$  should be constructed from the right eigenvector and left eigenvector, which satisfy

$$H(k)|\psi_m^R\rangle = E_m|\psi_m^R\rangle,$$

$$\langle \psi_m^L|H(k) = E_m\langle \psi_m^L|.$$
(A.4)

For our SSH chain model with long-range couplings, the right eigenvector and left eigenvector are calculated as

$$|\psi_{1,2}^{R}\rangle = \frac{1}{\sqrt{2}} \left( \pm \frac{\sqrt{h_a(k)h_b(k)}}{h_b(k)} \right),$$

$$|\psi_{1,2}^{L}\rangle = \frac{1}{\sqrt{2}} \left( \pm \left( \frac{\sqrt{h_a(k)h_b(k)}}{h_a(k)} \right)^* \right),$$
(A.5)

which satisfy the biorthogonal relation that  $\langle \psi_m^L | \psi_n^R \rangle = \delta_{mn}$ . The form of  $\rho$  and its inverse  $\rho^{-1}$  are derived as

$$\rho = |\psi_1^L\rangle\langle\psi_1^L| + |\psi_2^L\rangle\langle\psi_2^L| = \begin{pmatrix} |\frac{\sqrt{h_a(k)h_b(k)}}{h_a(k)}|^2 & 0\\ 0 & 1 \end{pmatrix},$$

$$\rho^{-1} = |\psi_1^R\rangle\langle\psi_1^R| + |\psi_2^R\rangle\langle\psi_2^R| = \begin{pmatrix} |\frac{\sqrt{h_a(k)h_b(k)}}{h_b(k)}|^2 & 0\\ 0 & 1 \end{pmatrix}.$$
(A.6)

Therefore,  $H^{\dagger}(k) = \rho H(k) \rho^{-1}$  requires that

$$h_a^*(k)h_b^*(k) = |h_a(k)h_b(k)|.$$
 (A.7)

Obviously, when  $h_a(k)h_b(k) \ge 0$ , the Bloch Hamiltonian has purely real spectrum, which is the so-called pseudo-Hermitian unbroken phase.

# References

- [1] Bender C M and Boettcher S 1998 Phys. Rev. Lett. 80(24) 5243-5246
- [2] El-Ganainy R, Makris K G, Khajavikhan M, Musslimani Z H, Rotter S and Christodoulides D N 2018 Nat. Phys. 14 11–19
- [3] Mostafazadeh A 2002 J. Math. Phys. 43 205–214
- [4] Mostafazadeh A 2002 J. Math. Phys. 43 2814–2816
- [5] Feshbach H 1958 Ann. Phys. 5 357–390 ISSN 0003-4916
- [6] Lindblad G 1976 Commun. Math. Phys. 48 119 130
- [7] Colbert D T and Miller W H 1992 J. Chem. Phys. **96** 1982–1991
- [8] Zhu X, Wang H, Gupta S K, Zhang H, Xie B, Lu M and Chen Y 2020 Phys. Rev. Research 2(1) 013280
- [9] Zhong J, Wang K, Park Y, Asadchy V, Wojcik C C, Dutt A and Fan S 2021 Phys. Rev. B 104(12) 125416
- [10] Zhang X, Tian Y, Jiang J H, Lu M H and Chen Y F 2021 Nat. Commun. 12 5377
- [11] Wang K, Dutt A, Yang K Y, Wojcik C C, Vučković J and Fan S 2021 Science 371 1240–1245
- [12] Parto M, Liu Y G N, Bahari B, Khajavikhan M and Christodoulides D N 2021 Nanophotonics 10 403–423
- [13] Yoshida T, Mizoguchi T and Hatsugai Y 2020 Phys. Rev. Research 2(2) 022062

- [14] Hofmann T, Helbig T, Schindler F, Salgo N, Brzezińska M, Greiter M, Kiessling T, Wolf D, Vollhardt A, Kabaši A, Lee C H, Bilušić A, Thomale R and Neupert T 2020 Phys. Rev. Research 2(2) 023265
- [15] Xu K, Zhang X, Luo K, Yu R, Li D and Zhang H 2021 Phys. Rev. B 103(12) 125411
- [16] Zhang X, Xu K, Liu C, Song X, Hou B, Yu R, Zhang H, Li D and Li J 2021 Commun. Phys. 4
- [17] Zou D, Chen T, He W, Bao J, Lee C H, Sun H and Zhang X 2021 Nat. Commun. 12 7201
- [18] Zhu W, Fang X, Li D, Sun Y, Li Y, Jing Y and Chen H 2018 Phys. Rev. Lett. 121(12) 124501
- [19] Zhang L, Yang Y, Ge Y, Guan Y J, Chen Q, Yan Q, Chen F, Xi R, Li Y, Jia D, Yuan S Q, Sun H X, Chen H and Zhang B 2021 Nat. Commun. 12 6297
- [20] Flebus B, Duine R A and Hurst H M 2020 Phys. Rev. B 102(18) 180408
- [21] Deng K and Flebus B 2022 Phys. Rev. B 105(18) L180406
- [22] Heiss W D 2004 J. Phys. A: Math. Gen. 37 2455–2464
- [23] Bender C M 2007 Rep. Prog. Phys. **70** 947–1018
- [24] Chen W, Kaya Özdemir S, Zhao G, Wiersig J and Yang L 2017 Nature 548 192–196 ISSN 1476-4687
- [25] Gong Z, Ashida Y, Kawabata K, Takasan K, Higashikawa S and Ueda M 2018 Phys. Rev. X 8(3) 031079
- [26] Ghatak A and Das T 2019 J. Phys.: Condens. Matter **31** 263001
- [27] Ashida Y, Gong Z and Ueda M 2020 Adv. Phys. 69 249-435
- [28] Bergholtz E J, Budich J C and Kunst F K 2021 Rev. Mod. Phys. 93(1) 015005
- [29] Klitzing K v, Dorda G and Pepper M 1980 Phys. Rev. Lett. 45(6) 494-497
- [30] Thouless D J, Kohmoto M, Nightingale M P and den Nijs M 1982 Phys. Rev. Lett. 49(6) 405–408
- [31] Hatsugai Y 1993 Phys. Rev. Lett. **71**(22) 3697–3700
- [32] Bernevig B A, Hughes T L and Zhang S C 2006 Science **314** 1757–1761
- [33] Schnyder A P, Ryu S, Furusaki A and Ludwig A W W 2008 Phys. Rev. B 78(19) 195125
- [34] Lee T E 2016 Phys. Rev. Lett. **116**(13) 133903
- [35] Yao S and Wang Z 2018 Phys. Rev. Lett. 121(8) 086803
- [36] Martinez Alvarez V M, Barrios Vargas J E and Foa Torres L E F 2018 Phys. Rev. B 97(12) 121401
- [37] Okuma N, Kawabata K, Shiozaki K and Sato M 2020 Phys. Rev. Lett. 124(8) 086801
- [38] Yokomizo K and Murakami S 2021 Phys. Rev. B 104(16) 165117
- [39] Kim K M and Park M J 2021 Phys. Rev. B **104**(12) L121101
- [40] Brody D C 2013 J. Phys. A: Math. Theor. 47 035305
- [41] Yao S, Song F and Wang Z 2018 Phys. Rev. Lett. 121(13) 136802
- [42] Yokomizo K and Murakami S 2019 Phys. Rev. Lett. 123(6) 066404
- [43] Kawabata K, Okuma N and Sato M 2020 Phys. Rev. B 101(19) 195147
- [44] Yang Z, Zhang K, Fang C and Hu J 2020 Phys. Rev. Lett. 125(22) 226402
- [45] Kunst F K and Dwivedi V 2019 Phys. Rev. B 99(24) 245116
- [46] Guo C X, Liu C H, Zhao X M, Liu Y and Chen S 2021 Phys. Rev. Lett. 127(11) 116801
- [47] Guo G F, Bao X X and Tan L 2021 New J. Phys. 23 123007
- [48] Liu Y, Zeng Y, Li L and Chen S 2021 Phys. Rev. B 104(8) 085401
- [49] Alase A, Cobanera E, Ortiz G and Viola L 2016 Phys. Rev. Lett. 117(7) 076804
- [50] Alase A, Cobanera E, Ortiz G and Viola L 2017 Phys. Rev. B 96(19) 195133
- [51] Mostafazadeh A and Batal A 2004 J. Phys. A: Math. Gen. 37 11645–11679